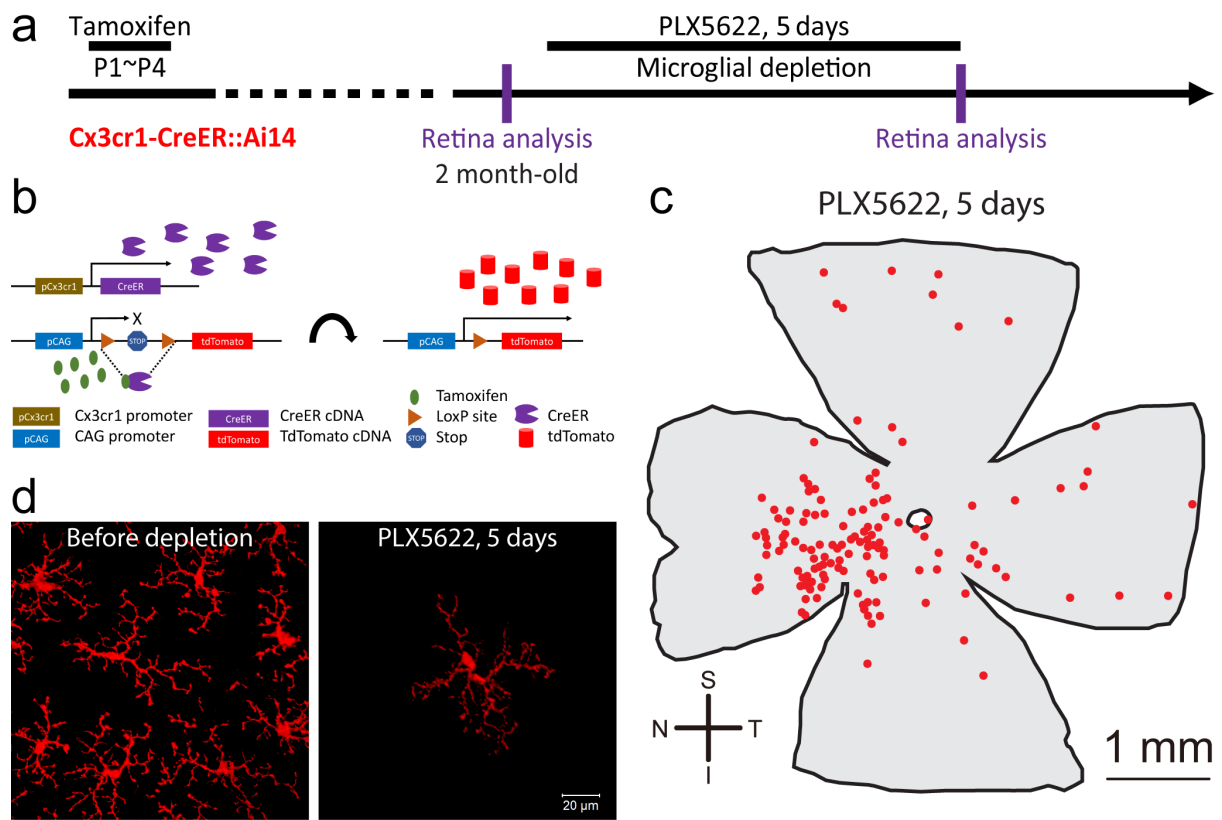
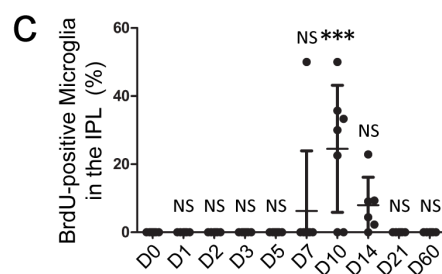
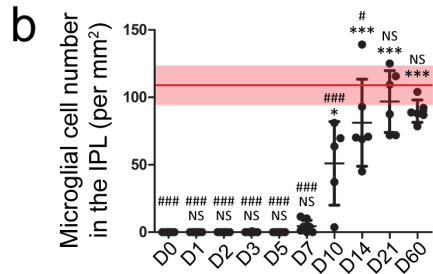
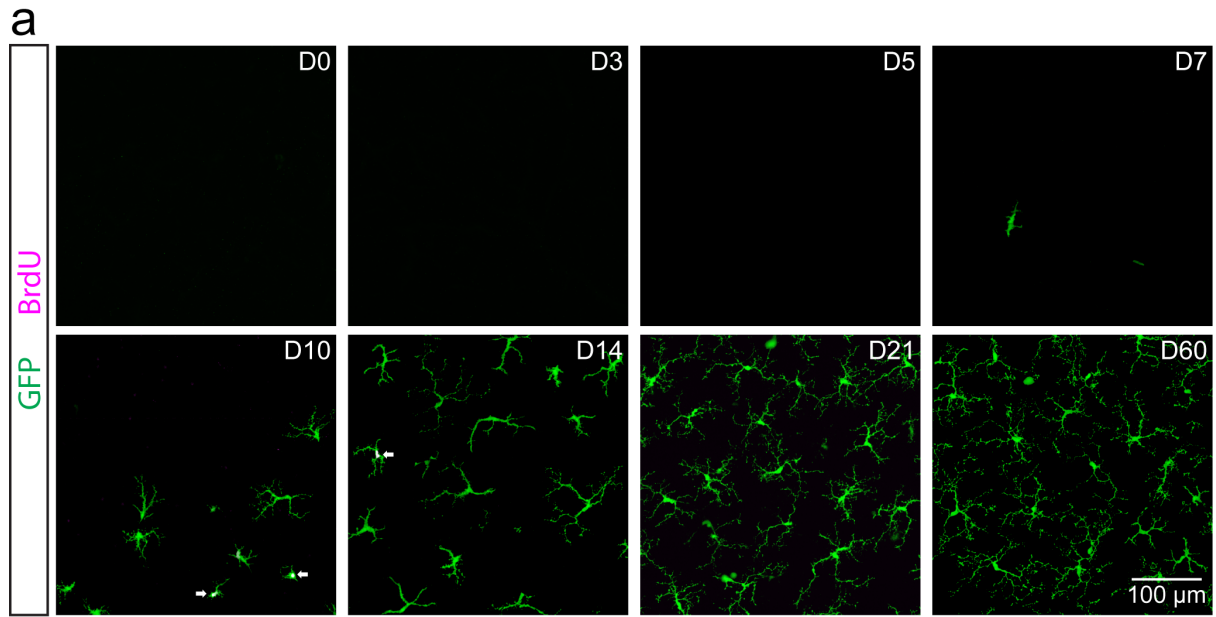


1  
2 **Supplementary Figure 1**  
3



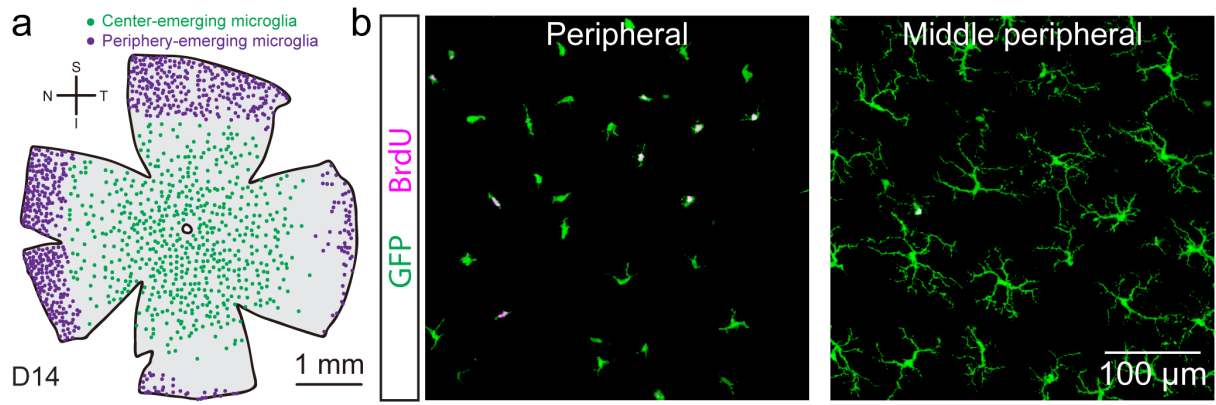
Supplementary Figure 2

1  
2  
3  
4



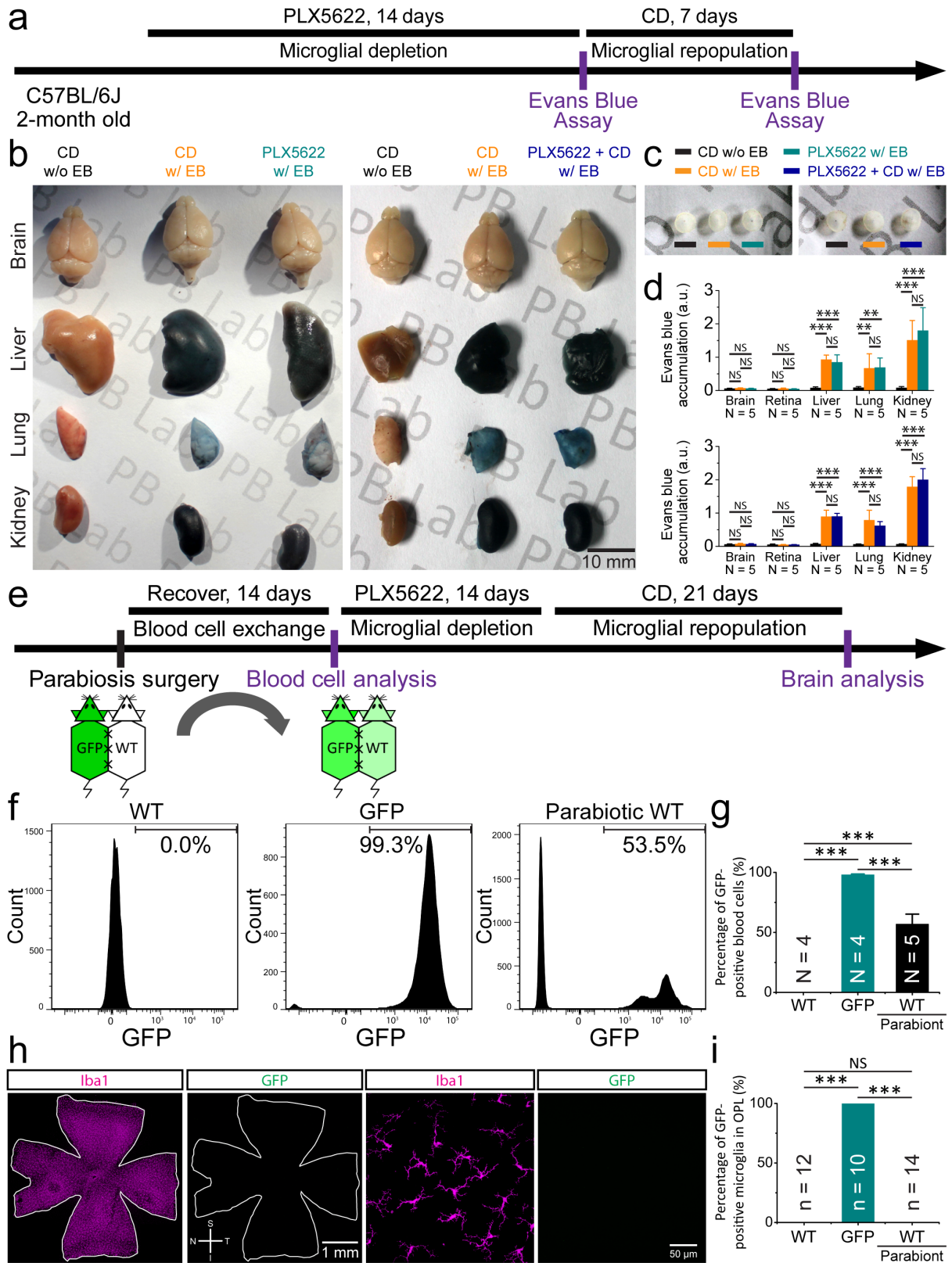
Supplementary Figure 3

1  
2  
3  
4  
5



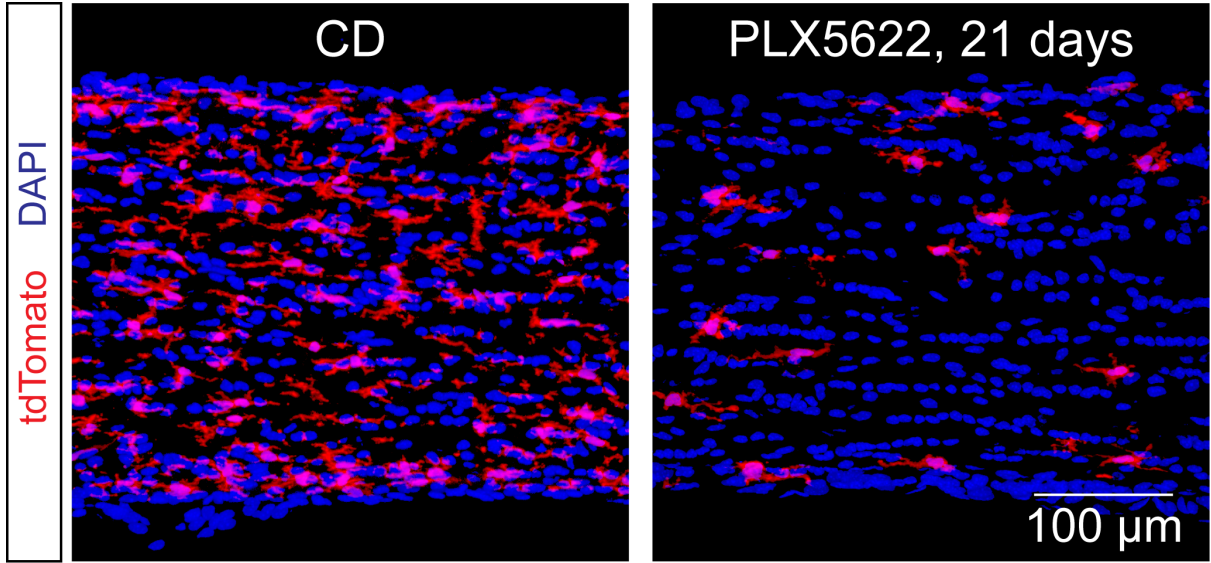
**Supplementary Figure 4**

- 1
- 2
- 3
- 4
- 5



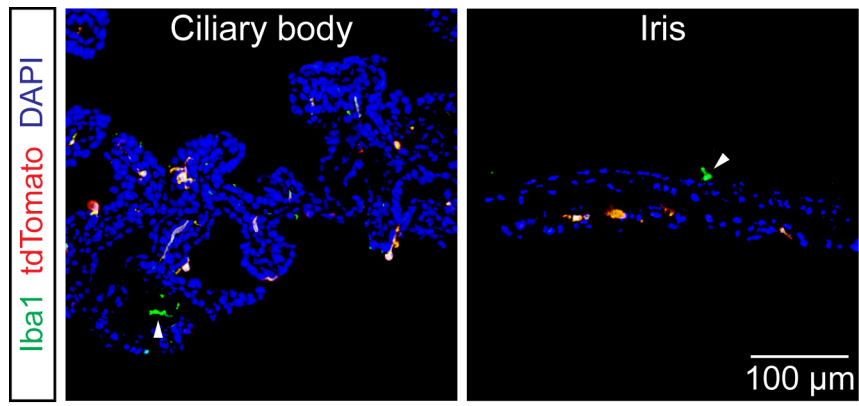
Supplementary Figure 5

1  
2  
3  
4



Supplementary Figure 6

- 1
- 2
- 3
- 4
- 5



1  
2  
3  
4  
5

Supplementary Figure 7

1 **Supplementary Figure Legends**

2 **Supplementary Figure 1** Inhibition of CSF1R by PLX5622 completely depletes microglia in  
3 IPL of the retina.

4 **(a)** Representative confocal images show microglial numbers are declined in the IPL of the  
5 retina after PLX5622 administration.

6 **(b)** Quantification of microglial density in the IPL of normal retinas and the retinas upon  
7 PLX5622 treatment.

8 S: superior; I: inferior; N: nasal; T: temporal; PLX5622: PLX5622 formulated diet. Green:  
9 GFP. The data are presented as mean  $\pm$  SD; NS: not significant; \*:  $p < 0.05$  to D0; \*\*:  $p < 0.01$   
10 to D0; \*\*\*:  $p < 0.001$  to D0. One-way ANOVA with Bonferroni's *post hoc*.

11

12

13

1 **Supplementary Figure 2** Retinal microglia are indeed depleted upon PLX5622 treatment.  
2 **(a)** Scheme of genetic inducible fate mapping for resident retinal microglia.  
3 **(b)** The rationale of tamoxifen-triggered fate mapping.  
4 **(c)** The spatial distribution of retinal microglia shows that the cell number is largely reduced  
5 after PLX5622 administration. Each red dot represents a tdTomato-positive cell.  
6 **(d)** Representative confocal images show that tdTomato-positive cell number is reduced in the  
7 retina after PLX5622 administration for 5 days.  
8 S: superior; I: inferior; N: nasal; T: temporal; PLX5622: PLX5622 formulated diet. Red:  
9 tdTomato.

10

11

12

1 **Supplementary Figure 3** Repopulated microglia replenish the IPL after removal of CSF1R  
2 inhibition.

3 **(a)** Representative confocal images show microglia emerge in IPL after removal of PLX5622.

4 **(b)** Quantification of microglial density in the IPL of the retina during microglial repopulation.

5 The red line and pink area indicate the mean and SD of microglial density in the normal retina,

6 respectively. NS: not significant; \*:  $p < 0.05$  to D0; \*\*:  $p < 0.01$  to D0; \*\*\*:  $p < 0.001$  to D0;

7 #:  $p < 0.05$  to the normal retina; ##:  $p < 0.01$  to the normal retina; ###:  $p < 0.001$  to the normal

8 retina.

9 **(c)** Quantification of BrdU-positive microglia in the IPL during repopulation. NS: not

10 significant; \*:  $p < 0.05$  to D0; \*\*:  $p < 0.01$  to D0; \*\*\*:  $p < 0.001$  to D0.

11 PLX5622: PLX5622 formulated diet; CD: control diet. Green: GFP; magenta: BrdU.

12 The data are presented as mean  $\pm$  SD. One-way ANOVA with Bonferroni's *post hoc*.

13

14

1 **Supplementary Figure 4** Two distinct populations of repopulated microglia in the retina.

2 **(a)** The representative spatial distribution of retinal microglia shows two distinct groups of  
3 microglia in the retina of repopulation for 10 days. Each green dot represents a center-emerging  
4 repopulated microglial cell, while each purple dot represents a periphery-emerging microglial  
5 cell.

6 **(b)** The periphery-emerging microglia in the peripheral retina exhibit distinct morphologies  
7 from center-emerging microglia in the middle peripheral retina.

8 S: superior; I: inferior; N: nasal; T: temporal. Green: GFP; magenta: BrdU.

9

10

1 **Supplementary Figure 5** Repopulated microglia in the retina are not derived from blood cells.

2 **(a)** Scheme and time points of Evans blue assay for the BRB/BBB integrity examination.

3 **(b-c)** Brains, peripheral organs (b) and retinas (c) from the microglia-depleted and microglia-  
4 repopulated mice 6 hours after Evans blue administration.

5 **(d)** Quantifications of the Evans blue intensity in retinas, brains and peripheral organs of  
6 microglia-depleted and microglia-repopulated mice.

7 **(e)** Scheme for testing the blood cell-derived pathway by parabiosis.

8 **(f-g)** Percentages of GFP-positive blood cells in the WT, beta-actin-GFP and WT parabiotic  
9 mice.

10 **(h)** Confocal images show that there are no GFP-positive repopulated microglia in the retina  
11 of WT parabionts.

12 **(i)** Quantifications of GFP-positive microglia in the OPL of the retinas in the WT, Cx3cr1<sup>+/GFP</sup>  
13 and parabiotic WT mice.

14 PLX5622: PLX5622 formulated diet; CD: control diet. Green: GFP; magenta: Iba1 (microglial  
15 marker). The data are presented as mean  $\pm$  SD. N: mouse number for each group; n: retina  
16 number for each group; NS: not significant; \*:  $p < 0.05$ ; \*\*:  $p < 0.01$ ; \*\*\*:  $p < 0.001$ . One-way  
17 ANOVA with Bonferroni's *post hoc*.

18

19

1 **Supplementary Figure 6** Microglia in the optic nerve are labeled by tdTomato in tamoxifen-  
2 treated Cx3cr1-CreER::Ai14 mice.  
3 Confocal images show that PLX5622 treatment for 21 days does not deplete all microglia in  
4 the optic nerve.  
5 Red: tdTomato; blue: DAPI.

6

7

1 **Supplementary Figure 7** Some macrophages in the ciliary body and iris are not labeled by  
2 tdTomato two months after tamoxifen injection.  
3 Confocal images show that some macrophages in the ciliary body and iris are not labeled by  
4 tdTomato two months after tamoxifen injection.  
5 Red: tdTomato; cyan: Iba1; green: Iba1; blue: DAPI. Arrow heads: tdTomato-negative  
6 macrophages.  
7